



CO₂ decomposition using the coaxial dielectric barrier discharge: effect of mixed gas and double outer electrodes

Nikom Rattanarojanakul^{1*} Somyos Srikhongrak², Witoon Nulek³ and Yutthana Tirawanichakul⁴

¹ Department of Physics and General Science, Faculty of Science and Technology, Rambhai Barni Rajabhat University, Chanthaburi, 22000, Thailand; nikom.p@rbru.ac.th
² Department of Physics and General Science, Faculty of Science and Technology, Rambhai Barni Rajabhat University, Chanthaburi, 22000, Thailand; somyos.s@rbru.ac.th
³ Department of Physics and General Science, Faculty of Science and Technology, Rambhai Barni Rajabhat University, Chanthaburi, 22000, Thailand; witoon.n@rbru.ac.th
⁴ Department of Physics, Faculty of Science, Prince of Songkla University, Songkhla, 90112, Thailand; yutthana.t@psu.ac.th
* Correspondence: nikom.p@rbru.ac.th

Citation:

Rattanarojanakul, N.;
Srikhongrak, S.; Nulek,
W.; Tirawanichakul, Y.
CO₂ decomposition using
the coaxial dielectric
barrier discharge: effect
of additive gas and
double outer electrodes.
ASEAN J. Sci. Tech.
Report. **2022**, 25(1), 50-59.
<https://doi.org/10.55164/ajstr.v25i1.244790>.

Article history:

Received: August 7, 2021
Revised: February 9, 2022
Accepted: February 11,
2022
Available online: March
29, 2022

Publisher's Note:

This article is published
and distributed under the
terms of the Thaksin
University.

Abstract: This work has studied CO₂ decomposition through the dielectric barrier discharge (DBD). The configuration of the DBD reactor was performed as a coaxial DBD tube. The dielectric barrier was made of a quartz tube with 1 mm thickness, while an outer electrode was made of a copper flat sheet wrapping around a quartz tube. The coaxial axis was made of stainless steel rod to be an inner electrode. The power source was applied by the alternative current (AC) high voltage with 7.8 kHz of frequency to both electrodes of the plasma reactor. The experiment was conducted on various conditions such as a mixed gas ratio, discharge gap, applied voltage, outer electrode length, two outer electrodes, and gas flow rate. The results showed that CO₂ conversion was decreased when CO₂ concentration increased. Similarly, the increase of gas flow rate also caused the decrease of CO₂ conversion. Whilst the increase of an applied voltage causes the CO₂ conversion clearly increased. Similarly, the CO₂:Ar ratio of 60%:40% achieved 30% of CO₂ conversion. Furthermore, the high percentage of CO₂ conversion of 47.2% has been obtained from a 1.3 mm discharge gap with 40 ml/min of gas flow rate.

Keywords: Gas conversions; DBD reactor; Pollution control; Gas discharges; Greenhouse Gases

1. Introduction

The dielectric barrier discharges (DBDs) are well-known for the generation of ionized gases and have been employed for several applications such as greenhouse gas decomposition, gas conversion, pollution control, ozone synthesis, excimer laser, material, and film surface modifications, etc. CO₂ gas is a part of greenhouse gases and has been attracting to the global warming and climate change on the earth, which can be more emitted from the transportations, burning of all fossil fuels, and also had presented in the natural gas and biogas [1-3]. However

CO_2 gas is one of the additive gases in the process of methane conversion into hydrocarbon gases [4-8]. The chemical bond of CO_2 is very strong and hard to be dissociated. To break the bond of C-O, the temperature has to be used at least at 1,500 °C for the thermolysis process, resulting in the huge power consumption. However, plasma technologies have been adopted to avoid the use of such high temperatures. Many geometries were configured for plasma-assisted reforming such as an arc discharge, glow discharge, corona discharge, dielectric barrier discharge (DBD), radio frequency (RF) discharge, etc. [9-18]. The reactions of plasma chemistry for CO_2 decomposition can be seen in Eq. 1 and Eq. 2, after the process of CO_2 decomposition, this CO_2 is converted into CO and O_2 [9-21]. Similarly, Eq. 1 and Eq. 2 confirm that CO and O_2 are the main product, where ΔH is the enthalpy of the reaction. However, O_2 can be formed by the recombination of O radicals, and similarly, CO_2 also has been reformed by the recombination of CO with O radicals and O_2 with C radicals [9, 22]. CO gas product is utilized for hydrocarbon fuel synthesis (e.g. methanol, ethanol, and acetic acid synthesis) and the mineral and metal industries (e.g. smelting and refining processing).



Furthermore, it can be considered in the unit of Joule [23].



The DBD plasmas have been utilized for a long time for surface modifications, gas treatment, chemical synthesis, etc. The characteristic of DBDs can initiate plasma reactions in low energy consumption and low temperature in the atmosphere. Whilst gas temperature can remain low, the electron temperature is high. These electrons have high energy in the range of 1-10 eV, in which it has enough energy to break the chemical bonds of gas molecules directly [9, 11, 24-28].

CO_2 conversion using a DBD reactor was operated under various conditions such as gas flow rate, gas temperature, power frequency, and power input [29]. The previous results indicated that the increase of input power and gas temperature could raise the conversion rate, while the increase of flow rate caused the conversion to decrease. In support, Indarto, A. et al. [9] had reported the review article for greenhouse gas and toxic gas decompositions via plasma technologies. In summary, they suggested that the advantage process should be the combined or new alternative process. In addition, other reports [9, 12, 14, 21] have also suggested and presented that noble gas (such as He, Ar, Kr, xe) contained in gas feeding or placing a solid catalyst in plasma zone can raise the rate of the gas conversion and product yield.

Furthermore, CO_2 was utilized in the process of CH_4 reforming to produce hydrogen and hydrocarbon fuels. A recent article from Tao, X. et al. [8] has reported the reviewed article for the opportunity of CH_4 - CO_2 reforming in different methods and processes. They have suggested that it is included by three factors to achieve high performance, there are reactor configuration, electron density, and plasma temperature. These factors caused the high plasma and electron densities to elevate the gas dissociation and produce more ions and neutron species.

This work represented CO_2 decomposition via the coaxial DBD applying by AC high voltage with high frequency under several conditions such as CO_2 mixed with Ar to increase an electron density [12, 14, 21], applied voltage, gas flow rate, discharge gap and discharge volume (length of outer electrode and outer electrode numbers). Which was operated in the atmosphere and the room temperature.

2. Materials and Methods

2.1. Experimental configuration

The experimental diagram is represented in Figure 1 consisting of CO_2 and Ar gas tanks, gas regulator, valve, flow meter, mixer unit, needle valve, coaxial DBD reactor, bubble flow meter, high

voltage power source, resistor ($R_{\text{limit}} = 1.5 \text{ k}\Omega$), measuring capacitor ($C_m = 10 \text{ nF}$), high voltage (HV) probe (Tektronix, P6015A), voltage probe, Oscilloscope (Tektronix, TDS3014B) and Gas analyzer (Geotech, Biogas Check). Coaxial DBD reactor was fabricated from quartz tube, Teflon insulator, Aluminum flat sheet, and stainless steel rod. A quartz tube with a thickness of 1 mm and an inner diameter of 12 mm was provided for a chamber. Teflon insulator is used for closing both sides of a quartz tube and fixing the inner electrode in the middle of a quartz tube. An aluminum flat sheet is wrapped around a quartz tube to set as an outer electrode, while stainless steel rod is placed inside of a quartz tube to be an inner electrode. Especially, Figure 2 has been illustrated the different installations for one outer electrode (A), two outer electrodes to increase the discharge volume (B), and the cross-section of the reactor (C).

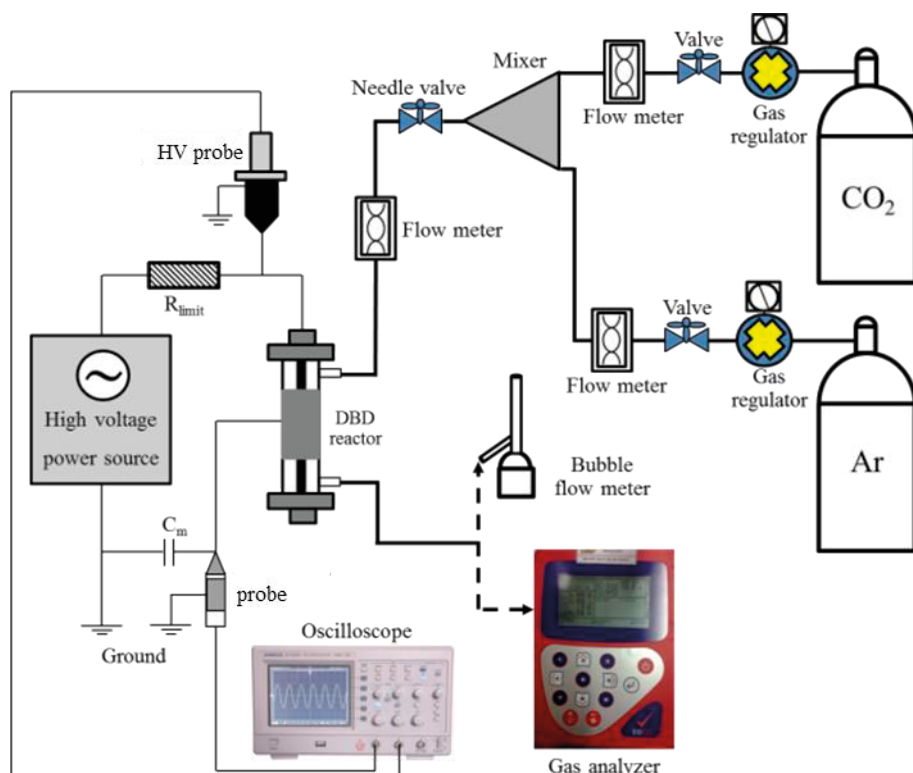


Figure 1. Experimental diagram and setup.



Figure 2. Reactor configuration for one outer electrode (A), two outer electrodes (B), and the cross-section of the reactor (C).

2.2. Operating and Measurement Methods

The concentration of CO_2 gas before and after the reaction process through the coaxial DBD reactor was investigated by a Gas analyzer instrument (Geotech, Biogas Check), this instrument consists of a gas detector for CH_4 , CO_2 , O_2 , and H_2S . Inlet gas flow was controlled and measured by a needle valve and flow meter, respectively, while outlet gas flow was measured by the bubble flow meter. The

applied voltage used for plasma generation is measured by the HV probe. Furthermore, charge transfer can be measured from the voltage across C_m by using a voltage probe. These parameters of applied voltage and charge transfer were utilized to calculate the power consumption by Q-U Lissajous plotting [30].

2.3. Analysis and Calculation Methods

The results will be analyzed such as CO_2 conversion (χ_{conv}), O_2 selectivity (O_{2s}), power consumption, and conversion efficiency to propose the performance for the system of CO_2 decomposition. The formulas for gas analysis are rewritten from Danhua, M. et al. [24] and Paulusen, S. et al. [29] as shown in the following equation.

$$\chi_{\text{conv}} (\%) = \frac{\text{CO}_2 \text{ converted (mol)}}{\text{CO}_2 \text{ input (mol)}} \times 100 \quad (4)$$

$$O_{2s} (\%) = \frac{\text{O}_2 \text{ product (mol)}}{\text{CO}_2 \text{ converted (mol)}} \times 100 \quad (5)$$

Whilst O_2 selectivity (O_{2s}) was calculated by Eq.5 because this O_2 molecule reformed from CO_2 dissociation. In the case of power consumption (P_E) and the conversion efficiency (η_{conv}), it can be adopted from Wang, S. et al. [10] and Phuengkum, N. et al. [30] as shown below.

$$P_E (W) = f \cdot C_m \int_0^T U_t du_c \quad (6)$$

$$\eta_{\text{conv}} (\% / W) = \frac{\text{CO}_2 \text{ conversion (\%)}}{P_E (W)} \quad (7)$$

In Eq. 6, parameters were included the power source frequency ($f = 7.8$ kHz), measuring capacitor ($C_m = 10$ nF), applied voltage (U_t) and voltage across C_m (u_c).

3. Results and Discussion

3.1. Effect of CO_2 concentrations

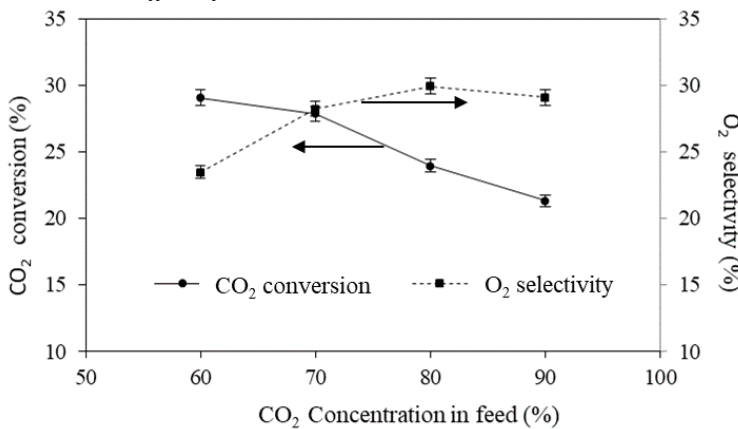


Figure 3. Effect of CO_2 diluted in Ar on CO_2 conversion and O_2 selectivity.

CO_2 gas was diluted by Ar gas, the percentage of CO_2 concentration was varied from 60% to 90%. The operating condition consists of 50 ml/min of gas flow rate, 1.30 mm of discharge gap, 8 cm of outer electrode length, and applied voltage was 8 kV. The result is shown in Figure 3, it has indicated that the increase of CO_2 concentration causes CO_2 conversion to decrease. On the other hand, O_2 selectivity which is the gas product has higher increased at 80% of CO_2 concentration.

3.2. Effect of outer electrode length and applied voltage

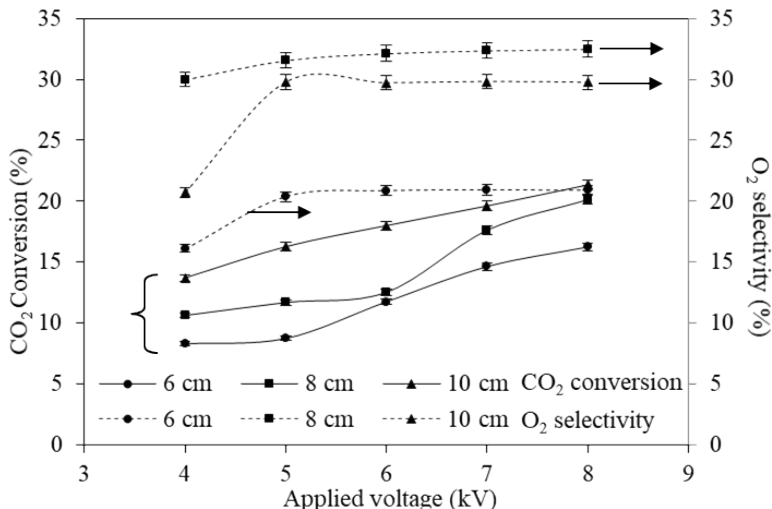


Figure 4. Effect of outer electrode length and applied voltage on CO₂ conversion and O₂ selectivity at 1.3 mm of discharge gap.

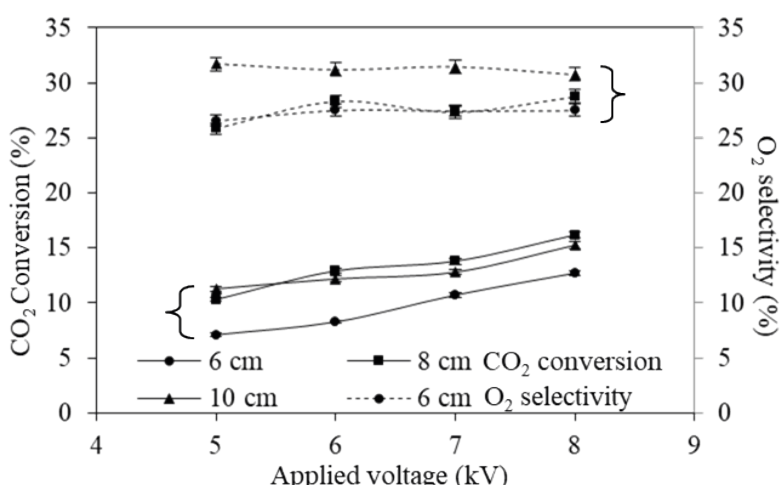


Figure 5. Effect of outer electrode length and applied voltage on CO₂ conversion and O₂ selectivity at 2.8 mm of discharge gap.

The experimental condition was conducted by 80 ml/min of gas flow rate and 60%:40% of CO₂:Ar ratio. These conditions have operated on two discharge gaps; there are 1.3 mm (Figure 4) and 2.8 mm (Figure 5), respectively. Figure 4 shows that the highest conversion of CO₂ can be achieved from the longest outer electrode. When the discharge gap is considered, 1.3 mm of discharge gap can raise CO₂ conversion higher than 15% for 8 cm and 10 cm of outer electrode lengths. In contrast, when the discharge gap was set at 2.8 mm (in Figure 5), the result has represented that it cannot raise CO₂ conversion to 15% for all of the outer electrode lengths. However, Figure 4 had been shown that 10 cm of outer electrode length can achieve higher CO₂ conversion than all of it. Whilst O₂ product was considered in terms of O₂ selectivity, Figure 4 and Figure 5 have indicated that O₂ selectivity was slightly changed after 5 kV of applied voltage. Indeed, it was implied that the high conversion of CO₂ can't raise the O₂ selectivity directly. As the gas product of CO₂ plasma consists of CO, O₂, and O₃, when O₂ selectivity was decreased it seems that the O₃ product might be increased. Because the O₃ forming can become from the recombination of O₂ molecules with O radicals.

3.3. Effect of discharge gap and plasma volume

The discharge gap is varied as 0.4 mm, 1.3 mm, and 2.8 mm, the length of the outer electrode was 8 cm, gas flow rate and CO₂:Ar ratio were 50 ml/min and 80%:20%, respectively. The free space between one outer electrode and another outer electrode was 8 cm as shown in Figure 2B to configure the two outer electrodes to increase the plasma volume. The result in Figure 6 has obviously indicated that the highest conversion of CO₂ can be obtained from the two outer electrodes with 1.3 mm of discharge gap (1.3 mm, 2OE). For O₂ selectivity, the result in Figure 7 has shown that O₂ selectivity from the 1.3 mm discharge gap with two outer electrodes (1.3 mm, 2OE) and 0.4 mm discharge gap has downward trended, while CO₂ conversion was increasing. However, the result in Figure 6 and Figure 7 have represented that the highest conversion of CO₂ and lowest O₂ selectivity can be achieved from a 1.3 mm discharge gap with two outer electrodes.

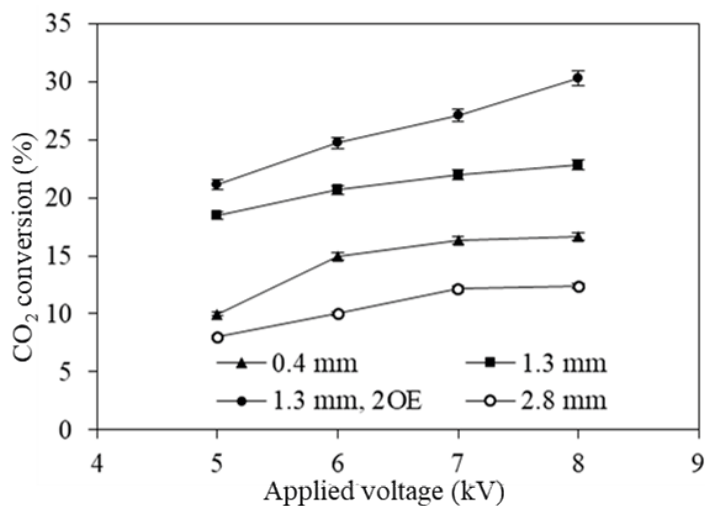


Figure 6. Effect of discharge gap and two outer electrodes (1.3 mm, 2 OE) on CO₂ conversion.

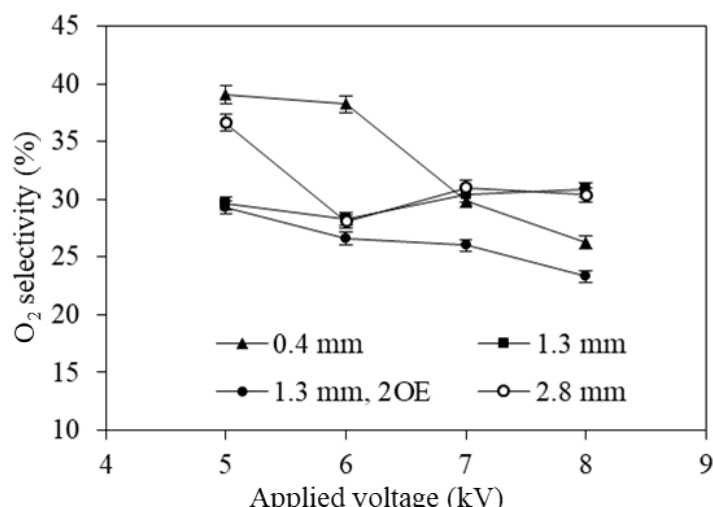


Figure 7. Effect of discharge gap and two outer electrodes (1.3 mm, 2 OE) on O₂ selectivity.

3.4. Effect of feeding flow rate

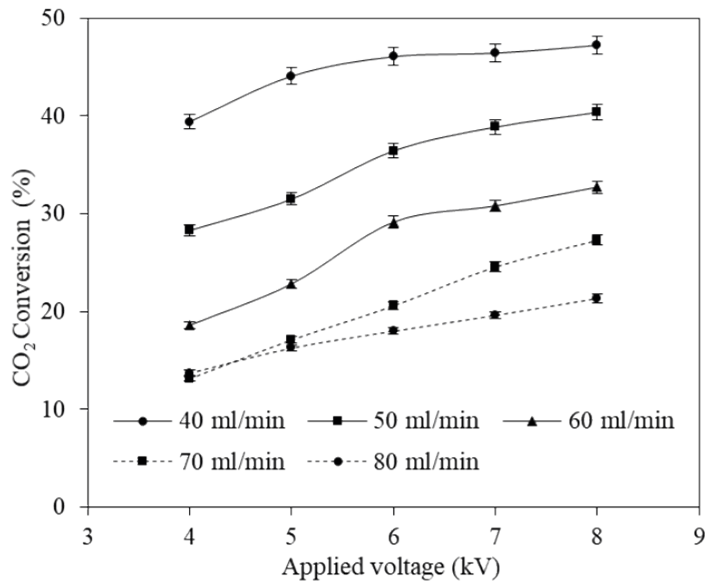


Figure 8. Effect of gas flow rate and applied voltage on CO₂ conversion and O₂ selectivity.

The experiment was conducted through the condition of 1.3 mm discharge gap, 60%:40% of CO₂:Ar ratio, 10 cm of outer electrode length. Whilst the feeding flow rate is varied from 40 ml/min to 80 ml/min. The result is shown in Figure 8, it has clearly present that the high flow rate causes the conversion CO₂ to decrease, while the low flow rate raises the percentage of CO₂ conversion. The highest conversion of CO₂ was obtained at 40 ml/min and gradually increased with increasing applied voltage.

3.5. Power consumption and conversion efficiency

The results were computed by Eq. 6 and Eq. 7 and have represented in Figure 9 and Figure 10 for the power consumption and conversion efficiency, respectively. In Figure 9, the results have shown that increasing of applied voltage causes the power consumption to increase for all conditions, while figure 10 has been showing the conversion efficiency was decreased when an applied voltage increased. However, the result has indicated that the high efficiency of CO₂ conversion can be achieved at a 1.3 mm discharge gap and 1.3 mm discharge gap with two outer electrodes. In contrast, the 2.8 mm discharge gap has shown a negative result of the power consumption and the conversion efficiency, there is high power consumption and low conversion efficiency.

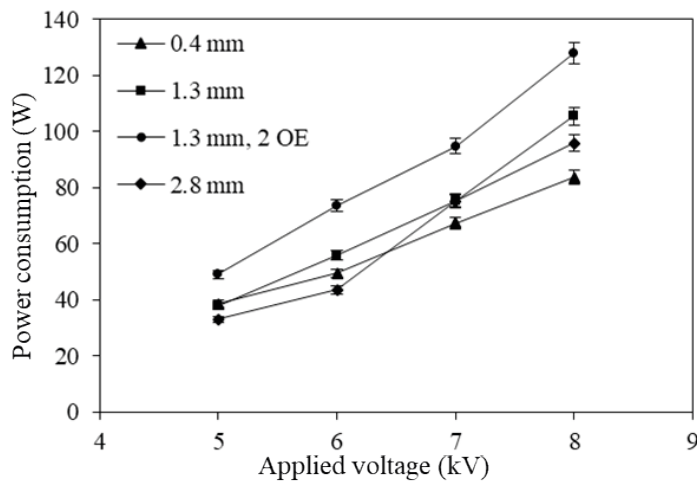


Figure 9. Power consumption versus applied voltage for each discharge gap.

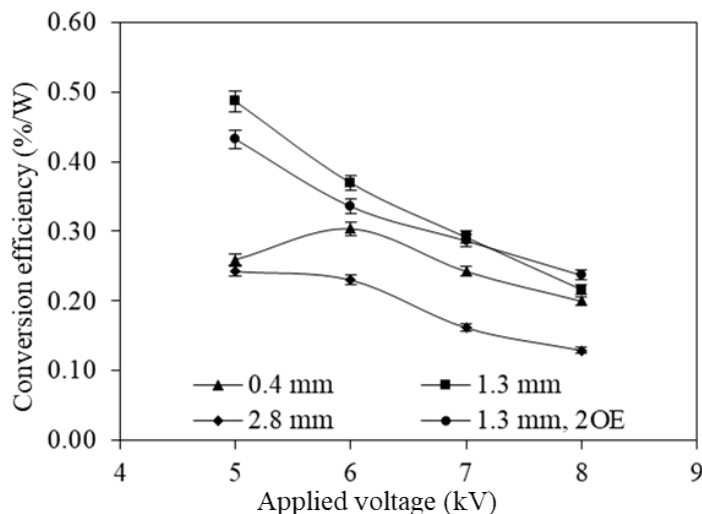


Figure 10. Conversion efficiency versus applied voltage for each discharge gap.

4. Conclusions

In summary, this work obviously exhibited that the use of the longest outer electrode at 10 cm and two outer electrodes with a 1.3 mm discharge gap could improve the performance of the coaxial DBD reactor and enhance the percentage of CO₂ conversion. In similarity, the increased applied voltage, low flow rate of gas feeding, and low CO₂ concentration can also raise the CO₂ conversion. It is clear that the highest percentage of CO₂ conversion was achieved at a 1.3 mm discharge gap with two outer electrodes, while its conversion efficiency was found to be lower than that of one outer electrode. In addition, this work can elevate the CO₂ conversion up to 47.2% at 10 cm of outer electrode length with a 1.3 mm discharge gap and 60%: 40% of the CO₂:Ar ratio with 40 ml/min of gas flow rate.

5. Acknowledgements

The authors would like to acknowledge to Faculty of Science and Technology and Rambhai Barni Rajabhat University for their support. Assist. Prof. Dr. Laemthong Chuenchom is thanked for proofreading the revised manuscript.

Author Contributions: IV characteristics of CO₂ and O₂ dielectric barrier discharges

Funding:

Conflicts of Interest:

References

- [1] Guangyin, Z.; Youcai, Z. *Pollution Control and Resource Recovery for Sewage Sludge*, Guangyin, Z., Youcai, Z., Eds.; Butterworth-Heinemann, 2017; pp. 352-275.
- [2] Da Costa Gomez, C. *The Biogas Handbook*, Wellinger, A., Murphy, J., Baxter, D., Eds.; Woodhead Publishing, 2013; pp. 1-16.
- [3] Lyon, D. R. *Environmental and Health Issues in Unconventional Oil and Gas Development*, Kaden, D., Rose, T., Eds.; Elsevier, 2016; pp. 33-48.
- [4] Rueangjitt, N.; Akarawitoo, C.; Chavadej, S. Production of Hydrogen-Rich Syngas from Biogas Reforming with Partial Oxidation Using a Multi-Stage AC Gliding Arc System. *Plasma Chemistry and Plasma Processing* 2012, pp. 583-596.
- [5] Kroker, T.; Kolb, T.; Schenk, A.; Krawczyk, K.; Mlotek, M.; Gericke, K.-H. Catalytic Conversion of Simulated Biogas Mixtures to Synthesis Gas in a Fluidized Bed Reactor Supported by a DBD. *Plasma Chemistry and Plasma Processing* 2012, pp. 1-18.
- [6] Kolb, T.; Kroker, T.; Voigt, J.; Gericke, K.-H. Wet Conversion of Methane and Carbon Dioxide in a DBD Reactor. *Plasma Chemistry and Plasma Processing* 2012, pp. 1-17.
- [7] Qi, W.; Huiling, S.; Binhang, Y.; Yong, J.; Yi, C. Steam enhanced carbon dioxide reforming of methane in DBD plasma reactor. *International Journal of Hydrogen Energy* 2011, pp. 8301-8306.
- [8] Tao, X.; Bai, M.; Li, X.; Long, H.; Shang, S.; Yin, Y.; Dai, X. CH₄-CO₂ reforming by plasma – challenges and opportunities. *Progress in Energy and Combustion Science* 2011, pp. 113-124.
- [9] Indarto, A.; Choi, J.-W.; Lee, H.; Song, H. K. Decomposition of greenhouse gases by plasma. *Environmental Chemistry Letters* 2008, pp. 215-222.
- [10] Wang, S.; Zhang, Y.; Liu, X.; Wang, X. Enhancement of CO₂ Conversion Rate and Conversion Efficiency by Homogeneous Discharges. *Plasma Chemistry and Plasma Processing* 2012, pp. 979-989.
- [11] Lee, D.; Kim, K.-T.; Song, Y.-H.; Kang, W.; Jo, S. Mapping Plasma Chemistry in Hydrocarbon Fuel Processing Processes. *Plasma Chemistry and Plasma Processing* 2012, pp. 1-21.
- [12] Indarto, A.; Yang, D> R.; Choi, J.-W.; Lee, H.; Song, H. K. Gliding arc plasma processing of CO₂ conversion. *Journal of Hazardous Materials* 2007, pp. 309-315.
- [13] Babaie, M.; Davari, P.; Talebizadeh, P.; Zare, F.; Rahimzadeh, H.; Ristovski, Z.; Brown, R. Performance evaluation of non-thermal plasma on particulate matter, ozone and CO₂ correlation for diesel exhaust emission reduction. *Chemical Engineering Journal* 2015, pp. 240-248.
- [14] Wen, Y.; Jiang, X. Decomposition of CO₂ Using Pulsed Corona Discharges Combined with Catalyst. *Plasma Chemistry and Plasma Processing* 2001, pp. 665-678.
- [15] Yoshida, K.; Rajanikanth, B. S.; Okubo, M. NO_x Reduction and Desorption Studies Under Electric Discharge Plasma Using a Simulated Gas Mixture: A Case Study on the Effect of Corona Electrodes. *Plasma Science and Technology* 2009, pp. 327-333.
- [16] Xiang, L.; Xumei, T.; Yongxiang, Y. An Atmospheric-Pressure Glow-Discharge Plasma Jet and Its Application. *IEEE Transaction on Plasma Science* 2009, pp. 759-763.
- [17] Chang, M. D.; Jian, H. Y.; Bruno, C. Decomposition of toluene in a gliding arc discharge plasma reactor. *Plasma Sources Science and Technology* 2007, pp. 791-799.
- [18] Xu, S.; Khalaf, P.; Martin, P.; Christopher, W. J. CO₂ dissociation in a packed-bed plasma reactor: Effects of operating conditions. *Plasma Science and Technology* 2018, Volume 27, pp. 1-13.
- [19] Fridman, A. *Plasma Chemistry*, Cambridge University Press: New York, 2008; p. 978.
- [20] Spencer, L.; Gallimore, A. Efficiency of CO₂ Dissociation in a Radio-Frequency Discharge. *Plasma Chemistry and Plasma Processing* 2011, pp. 79-89.
- [21] Mei, D.; Zhu, X.; Wu, C.; Ashford, B.; Williams, P. T.; Tu, X. Plasma-photocatalytic conversion of CO₂ at low temperatures: Understanding the synergistic effect of plasma-catalysis. *Applied Catalysis B: Environmental* 2016, Volume 182, pp. 525-532.
- [22] Yu, Q.; Kong, M.; Liu, T.; Fei, J.; Zheng, X. Characteristics of the Decomposition of CO₂ in a Dielectric Packed-Bed Plasma Reactor. *Plasma Chemistry and Plasma Processing* 2012, pp. 153-163.
- [23] Zheng, G.; Jiang, J.; Wu, Y.; Zhang, R.; Hou, H. The Mutual Conversion of CO₂ and CO in Dielectric Barrier Discharge (DBD). *Plasma Chemistry and Plasma Processing* 2003, pp. 59-68.

- [24] Danhua, M.; Xinbo, Z.; Ya-Ling, H.; Joseph, D. Y.; Xin, T. Plasma-assisted conversion of CO₂ in a dielectric barrier discharge reactor: understanding the effect of packing materials. *Plasma Sources Science and Technology* 2015, Volume 24, pp. 1-10.
- [25] Tendero, C.; Tixier, C.; Tristant P.; Desmaison, J.; Leprince, P. Atmospheric pressure plasmas: A review. *Spectrochimica Acta Part B: Atomic Spectroscopy* 2006, pp. 2-30.
- [26] Wagenaars, E.; Brandenburg, R.; Brok, W. J. M.; Bowden, M. D.; Wagner, H.-E. Experimental and modelling investigations of a dielectric barrier discharge in low-pressure argon. *Journal of Physics D: Applied Physics* 2006, pp. 700-711.
- [27] Wagner, H. E.; Brandenburg, R.; Kozlov, K. V.; Sonnenfeld, A.; Michel, P.; Behnke, J. F. The barrier discharge: basic properties and applications to surface treatment. *Vacuum* 2003, pp. 417-436. doi:10.1016/S0042-207X(02)00765-0.
- [28] Kogelschatz, U. Dielectric-Barrier Discharges: Their History, Discharge Physics, and Industrial Applications. *Plasma Chemistry and Plasma Processing* 2003, pp. 1-46.
- [29] Paulusen, S.; Verheyde, B.; Tu, X.; Bie, C. D.; Martens, T.; Petrovic D.; Bogaerts, A.; Sels, B. Conversion of carbon dioxide to value-added chemicals in atmospheric pressure dielectric barrier discharges. *Plasma Sources Science and Technology*, 2010; Volume 19, pp. 1-6.
- [30] Phuengkum, N.; Tirawanichakul, Y. Physics applications: IV characteristics of CO₂ and O₂ dielectric Barrier discharges. 2011 *IEEE Colloquium on Humanities, Science and Engineering (CHUSER)* 2011, pp. 805-808.